Electronic Structure and Magnetic Properties of New Rare-earth Half-metallic Materials AcFe$_2$O$_4$ and ThFe$_2$O$_4$: Ab Initio Investigation

Jingguo Yan[1], Xudong Wang[1], Man Yao[1,2] and Ning Hu[3,4]

Abstract: Electronic structure and magnetism of the rare-earth metals Ac and Th doped Fe$_3$O$_4$ Fe$_{1-x}$Re$_x$Fe$_{2-y}$Re$_y$O$_4$(Re=Ac, Th; x=0, 0.5, 1; y=0, 0.5, 1.0, 1.5, 2.0) are investigated by first-principle calculations. AcFe$_2$O$_4$, FeAc$_2$O$_4$ and ThFe$_2$O$_4$ are found to be II B-type half-metals. The large bonding-antibonding splitting is believed to be the origin of the gap for AcFe$_2$O$_4$, FeAc$_2$O$_4$ and ThFe$_2$O$_4$, resulting in a net magnetic moment of $9.0\mu_B$, $4.0\mu_B$ and $8.1\mu_B$, respectively, compared with $4.0\mu_B$ of Fe$_3$O$_4$. Also, the conductance of AcFe$_2$O$_4$ and ThFe$_2$O$_4$ are both slightly larger than that of Fe$_3$O$_4$. It can be predicted that the new rare-earth half-metals AcFe$_2$O$_4$ and ThFe$_2$O$_4$ have wider application ground in spin electronic devices due to their larger magnetoresistance and higher conductivity than that of Fe$_3$O$_4$. The half-metallic feature can be maintained up to the lattice contraction of 8%, 3% and 4% for Fe$_3$O$_4$, AcFe$_2$O$_4$ and ThFe$_2$O$_4$, respectively.

Keywords: Half-metallicity, first-principle, AcFe$_2$O$_4$, ThFe$_2$O$_4$, electronic structure, magnetic moment.

1 Introduction

Half-metals, as a new kind of ideal spintronic functional materials, have drawn much attention due to their 100% spin polarization at the Fermi level and being able to control the spins of electrons and transmission of charges simultaneously to realize efficient information storage and processing [de Groot *et al.* (1983); Prinz (1999); Coey *et al.* (2002); Kopcewicz *et al.* (2005); Tan *et al.* (2012); Zhao *et al.* (2012)]. Compared to ordinary semiconductor electronic devices, devices

---

[1] School of Materials Science and Engineering, Dalian University of Technology, Dalian, China.

[2] Corresponding author: Man Yao. Email: yaoman@dlut.edu.cn

[3] Department of Engineering Mechanics, College of Aerospace Engineering, Chongqing University, Chongqing, China.

[4] Corresponding author: Ning Hu. Email: ninghu@cqu.edu.cn or huning@faculty.chiba-u.jp

made of half-metals have such outstanding features as non-volatile, low power consumption and high integration. What's more, more dimensions considered in the research of half-metal materials will produce more new excellent properties and more applications [Wolf *et al*. (2001); Ming *et al*. (2012); Yao *et al*.(2012)]. To date, many half-metals have been found experimentally and theoretically [Coey *et al*. (2002); Dedkow *et al*. (2002); Fong *et al*. (2004); Hou *et al*. (2011); Chen *et al*. (2012)]. Among them, the II B-type half-metal Fe_3O_4 has attracted much more attention due to their special advantages, such as stable performance, larger room-temperature spin-polarization, higher courier temperature, easy preparation [Kim *et al*. (2003)]. However, its magnetoresistance is not large enough to give access to huge magnetoresistance effects when used as magnetic electrodes in spintronic devices. Consequently, it is an urgent mission to design new spinel half-metals with larger magnetoresistance and higher conductivity.

First principle calculation has been a very effective method to predict and analyze the properties of crystal materials and many Fe_3O_4 based half-metals have been designed by this method [Liu, Chen *et al*. (2007); Liu, Wang *et al*. (2007); Liu *et al*. (2008)]. However, this research effort is still in the initial stage of exploration. Many micromechanisms about spinel half-metals is still unknown, especially exploration of doping effect of rare-earth metals on the half-metallicity of Fe_3O_4 is very limited.

In this paper, we will find out the doping effect of 6d transition rare-earth metals Ac and Th on the electronic structure and half-metallicity of Fe_3O_4 by first principle and manage to predict new spinel half-metals with more excellent properties.

2   Model and method

As shown in Fig.1 is a 14-atom primitive cell of Fe_3O_4 with two Fe atoms on A-sites and the other four on B-sites. Fe atoms were suitably doped by Ac or Th atoms with different concentration to form, namely, $Fe_{1-x}Re_xFe_{2-y}Re_yO_4$ (Re=Ac, Th; x=0, 0.5, 1; y=0, 0.5, 1.0, 1.5, 2.0). The subscript x represents the doping fraction of A-site Fe atoms while y B-site.

First principle calculation, also known as ab initio calculation, is based on the principles of quantum mechanism. It is mainly used to deal with the Hamilton equation, as shown in Eq.1.

$$\hat{H} = -\frac{\hbar^2}{2m_e}\sum_i \nabla_i^2 + \sum_{i,j}\frac{Z_j e^2}{\left|\vec{r}_i - \vec{R}_I\right|} + \frac{1}{2}\sum_{i\neq j}\frac{e^2}{\left|\vec{r}_i - \vec{r}_j\right|} - \sum_I \frac{\hbar^2}{2M_I}\nabla_I^2 + \frac{1}{2}\sum_{I,J}\frac{Z_I Z_J e^2}{\left|\vec{R}_I - \vec{R}_J\right|} \quad (1)$$

where on the right side of Eq.1, the parts from left to right represent the kinetic energy of electrons, the Coulomb potential energy between electrons and nucleus,
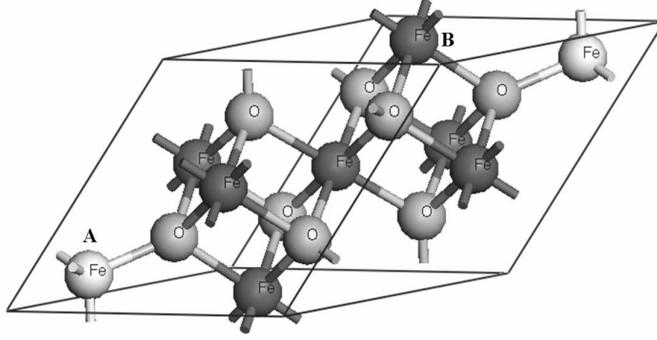
Figure 1: Primitive cell of Fe$_3$O$_4$.

interaction between electrons, kinetic energy of nucleus and Coulomb potential energy between nucleus, in which r and R represent the positions of the electron and nuclear respectively, Z the charge number of a nuclear, e the electronic charge, m and M the mass of the electron and nuclear. By self-consistent calculating electron motion and the interaction between electrons and nucleus, it can obtain the geometry structure, electronic, magnetic, thermodynamic properties of the materials [*Kohn et al.* (1965)]. To solve this equation, we need to use some approximations. Based on the Born-Oppenheimer approximation [*Born et al.* (1954)], density functional theory (DFT) [*Kohn et al.* (1965)] was proposed in which the ground state physical properties of electrons, atoms and materials are all functionalized by electron densities and the energy function E[ρ] is minimized by the electron density ρ(r). Based on Hohenberg-Kohn principle [*Hohenberg et al.* (1964)], the Hamilton energy H is divided into three parts: kinetic energy T, interaction energy between electrons V and external electric field energy U, as shown in Eq.2

$$H = T + V + U \tag{2}$$

Then with Φ presenting wave function the total energy function can be expressed as:

$$E[\rho] = \langle \Phi | T + V | \Phi \rangle + \int dr v(r) \rho(r) \tag{3}$$

Kohn and Sham further derived this equation and by introducing electron exchange and correlation function E$_{xc}$[ρ], the total energy function is expressed:

$$E(\rho) = \sum_{i=1}^{N} \int dr \Phi_i^*(\vec{r}) \left(-\nabla^2\right) \Phi_i(r) + \frac{1}{2} \iint dr dr' \frac{\rho(\vec{r}) \rho(\vec{r}')}{|\vec{r} - \vec{r}'|}$$
$$+ \int dr V(\vec{r}) \rho(\vec{r}) + E_{xc}[\rho] \tag{4}$$

Through Eq.5

$$\frac{\delta \sum_{i=1}^{N} \int dr \Phi_i^* (\vec{r}) (-\nabla^2) \Phi_i (r) + \frac{1}{2} \iint dr dr' \frac{\rho(\vec{r})\rho(\vec{r}')}{|\vec{r}-\vec{r}'|} + \int dr V (\vec{r}) \rho (\vec{r}) + E_{xc} [\rho]}{\delta \rho} = 0 \quad (5)$$

Kohn-Sham equation is derived as follows:

$$\left[-\nabla^2 + V_{KS} [\rho (\vec{r})] \right] \Phi_i (\vec{r}) = E_i \Phi_i (\vec{r}) \quad (6)$$

where

$$V_{KS} [\rho (r)] \equiv v(r) + \int dr' \frac{\rho (r')}{|r - r'|} + \frac{\delta E_{xc} (\rho)}{\delta \rho (r)} \quad (7)$$

$$\rho (r) = \sum_{i=1}^{N} |\Phi_i (r)|^2 \quad (8)$$

Finally the purpose of using DFT method to calculate the total energy of multiple electrons system and deal with charge density distribution is achieved.

We can see from Eq.6 that $E_{xc} [\rho]$ is the key for the accuracy of the calculating results.

Two approximation methods are used to treat $E_{xc} [\rho]$: Local Density Approximation (LDA) and Generalized Gradient Approximation (GGA) [Kohn *et al.* (1965)]. Electron density gradient is considered in GGA compared LDA, therefore, GGA is more suitable for treating systems with very large charge density fluctuation. Perdew-Wang 91 (PW91) and Perdew-Burke-Ernzerhof (PBE) etc. are all the parameterized formation for GGA.

In this paper, the spin-polarized structural optimization, electronic structure and magnetic moments calculations were performed with the PBE parameterized G-GA and projector augmented wave methods. The interaction between the valence electrons and ion cores were described by ultrasoft pseudo-potentials [Kresse *et al.* (1999)]. The self-consistent calculations were performed with a 5×5×5 k-mesh and the cutoff energy of plane-wave expansion was 500eV. The relaxations of lattices were performed until the force on each atom was smaller than 0.03eV/Å, and all components of the stress tensor on the unit cell less than 0.05GPa.

3   Results and Discussion

To obtain the equilibrium lattice constant and determine the stable magnetic state of $Fe_{1-x}Re_xFe_{2-y}Re_yO_4$ (Re=Ac, Th; x=0, 0.5, 1; y=0, 0.5, 1.0, 1.5, 2.0), for each structure, structural optimizations were performed for the nonmagnetic (NM),

ferromagnetic (FoM), ferrimagnetic (FiM) or antiferromagnetic (AFM) state. After optimization the structure of the lowest energy is believed to be stable with the corresponding lattice parameters and the corresponding magnetism. The electronic structure of the stable structure will then be calculated and their half-metallicity will also be determined.

3.1   Half-metallicity and Magnetic properties of Ac and Th doped Fe$_3$O$_4$

Among these structures, besides Fe$_3$O$_4$, only AcFe$_2$O$_4$, FeAc$_2$O$_4$ and ThFe$_2$O$_4$ are calculated to be half-metallic materials. Population analysis of the resulting half-metals is then performed using Mulliken formalism. Parameters listed in Table 1 are the equilibrium lattice constants and molecular (M$_s$) and atomic magnetic moments for Fe$_3$O$_4$, AcFe$_2$O$_4$, FeAc$_2$O$_4$ and ThFe$_2$O$_4$ within which M$_A$ means the A-site atom moment and M$_B$ the B-site atom moment. Our calculated molecular magnetic moment of Fe$_3$O$_4$ is 4.0 μ_B at equilibrium lattice constant 5.94Å, agrees quite well with other's [Liu, Chen *et al.* (2007)], which is 4.0 μ_B at 5.935Å. And M$_A$ is -3.60 μ_B while M$_B$ is 3.60μ_B, consistent with the reported characteristic that the A-site atoms have spin directions opposite to the B-site ones in Fe$_3$O$_4$, exhibiting ferromagnetic [Kim *et al.* (2007)], all conforming the accuracy of the method we used. In AcFe$_2$O$_4$, FeAc$_2$O$_4$ and ThFe$_2$O$_4$, there are almost no spin moments for Ac and Th due to only one and two 6d electrons, respectively. But the Fe atom magnetic moments in AcFe$_2$O$_4$, FeAc$_2$O$_4$ and ThFe$_2$O$_4$ are 3.90, 3.78 and 3.82μ_B, respectively, both slightly larger than that in Fe$_3$O$_4$. The impressive finding is that the calculated M$_s$ of AcFe$_2$O$_4$ and ThFe$_2$O$_4$ are 9.0μ_B and 8.1μ_B, much larger than that of Fe$_3$O$_4$. Higher magnetic molecule moment may cause stronger spin-correlation scattering for conductive electrons resulting in higher variation of resistance, and consequently obtaining higher magnetoresistance effects which is the key for spintronic devices.

Table 1: Calculated lattice constants, molecular and atomic magnetic moments for Fe$_3$O$_4$, AcFe$_2$O$_4$, FeAc$_2$O$_4$ and ThFe$_2$O$_4$.

Alloys	Lattice Constants(Å)	M$_s$(μ_B)	M$_A$(μ_B)	M$_B$(μ_B)	M$_O$(μ_B)
Fe$_3$O$_4$	5.94	4.0	-3.60	3.60	0.10
AcFe$_2$O$_4$	6.30	9.0	0.04	3.90	030
FeAc$_2$O$_4$	6.47	4.0	3.78	-0.02	0.08
ThFe$_2$O$_4$	6.41	8.1	-0.04	3.82	0.12

3.2   *Electronic structure of AcFe$_2$O$_4$ and ThFe$_2$O$_4$*

The total and partial spin-polarized density of states (DOS) of a) AcFe$_2$O$_4$ and b) ThFe$_2$O$_4$ are calculated and shown in Fig.2. We can see that there is much difference in DOS of up-spin and down-spin electrons near the Fermi energy level. Especially, at the Fermi level, the down-spin states cross the Fermi energy level, indicating a strong metallic nature of the spin-down electrons while the spin-up band structure exhibits a band gap indicating semiconducting nature. Therefore, our results reveal that AcFe$_2$O$_4$ and ThFe$_2$O$_4$ alloys exhibit half-metallic properties. The electrons are 100% spin-polarized for AcFe$_2$O$_4$ and almost 100% for ThFe$_2$O$_4$. High spin polarization is the base for high sensitivity of spintronic devices considering magnetoresistance effects. So they are of great interest for scientific research and industrial applications. To show the electronic structures in detail, we plotted the down-spin energy bands of a) Fe$_3$O$_4$, b) AcFe$_2$O$_4$ and c) down-spin and d) up-spin energy bands of ThFe$_2$O$_4$along high symmetry directions in the Brillouin zone in Fig.3. It is clear that the bottom of the conductance band touches the Fermi level at the G point but is rather weak, and the calculated spin-polarization for ThFe$_2$O$_4$is near 99%. Therefore, AcFe$_2$O$_4$ and ThFe$_2$O$_4$ are all considered to be typical II B-type half-metallic materials. Comparing the down-spin sub-bands of the three materials, we see that, there are some limited parabolas near the Fermi level meaning that electrons at the Fermi level are localized but not completely. And parabolas at both b) and c) are more clear than a), which means down-spin electrons of AcFe$_2$O$_4$ and ThFe$_2$O$_4$ at the Fermi level are less localized than that of Fe$_3$O$_4$. It is also seen that there is up-spin sub-bands in ThFe$_2$O$_4$. According to the two-fluid model of magnetoresistance effect, the up-spin and down-spin electrons transmit in parallel. So we believe that AcFe$_2$O$_4$ and ThFe$_2$O$_4$ both have higher conductivity than that of Fe$_3$O$_4$, and ThFe$_2$O$_4$ has the highest. Higher conductivity is very important for the transmission of charges in half-metallic materials which plays a significant role in effective function. So AcFe$_2$O$_4$ and ThFe$_2$O$_4$ may be better than Fe$_3$O$_4$ for spintronic devices.

We can see that for AcFe$_2$O$_4$ and ThFe$_2$O$_4$ in both majority and minority spin states, the total DOS are divided into bonding, nonbonding and antibonding states by an energy gap. The region from -7.2eV to -2.2eV corresponds to the bonding states, -1.8eV $\sim$ 0.9eV corresponds to the nonbonding states, states from 1.2eV to 6.3eV are associated with the antibonding states in AcFe$_2$O$_4$ while the bonding, nonbonding and antibonding states of ThFe$_2$O$_4$ are divided into -7.5eV $\sim$ -2.4eV region, -2.1eV $\sim$ 0.7eV region and 0.9eV $\sim$ 3.6eV region. So the band region of AcFe$_2$O$_4$ and ThFe$_2$O$_4$ are about 13.5eV and 12.1eV, respectively which are very broad. The broad bands for AcFe$_2$O$_4$ and ThFe$_2$O$_4$ stem from their greater dependence on bonding-antibonding splitting and less on exchange splitting. And
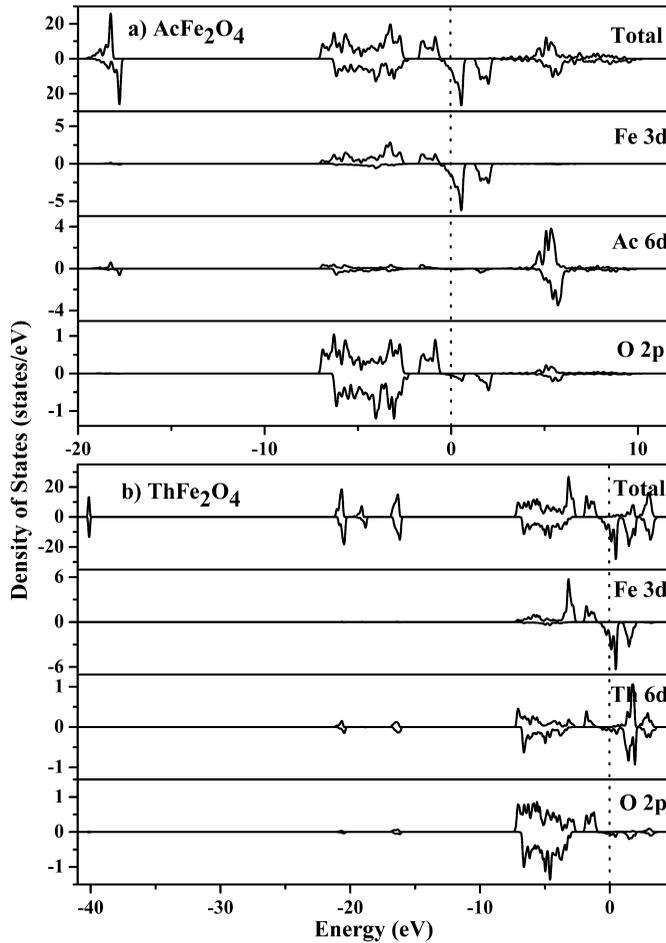
Figure 2: Total and partial DOS of a) AcFe$_2$O$_4$and b) ThFe$_2$O$_4$ at their stable states, the dotted line represent the Fermi level.

the large bonding-antibonding splitting is exactly the origin of the gap for AcFe$_2$O$_4$ and ThFe$_2$O$_4$.

What's more, for both AcFe$_2$O$_4$ and ThFe$_2$O$_4$, the partial DOS of Fe shows a two-peak structure due to the strong hybridization between the Fe 3d states, Ac or Th 6d state and O 2p states caused by the crystal field effect. In upspin, the antibonding peak is below the Fermi level and occupied, but in down spin the splitting effect moves the antibonding peak high above the Fermi level. This distribution results in a large magnetic moment at Fe and makes Fe 3d electrons mostly responsible for the magnetization. The Fe 3d down-spin states cross the Fermi level, so they also
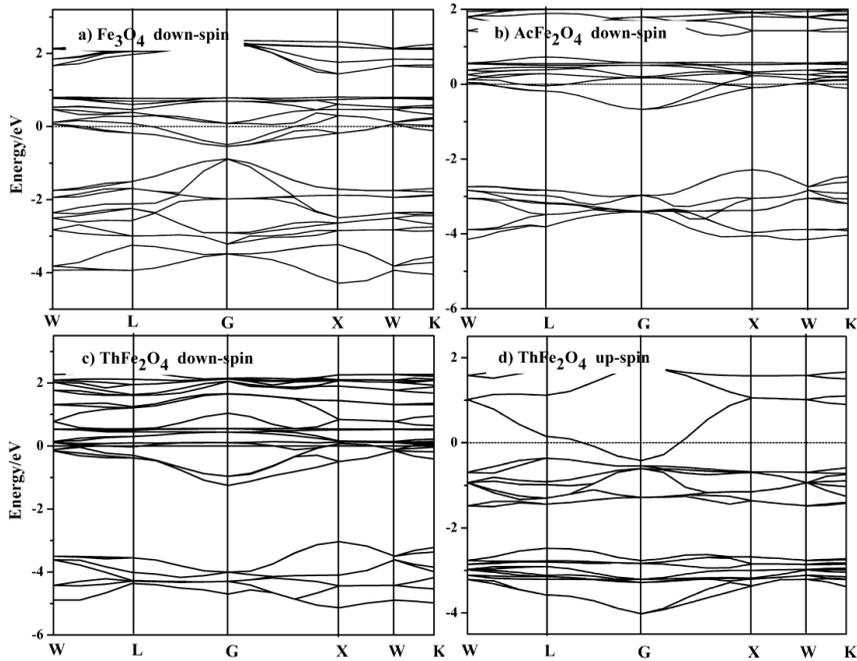
Figure 3: The energy band structure for Fe_3O_4, $AcFe_2O_4$ and $ThFe_2O_4$, where the horizontal lines at 0 eV represent the Fermi energy level.

have main contribution to the down-spin DOS at the Fermi level. The distribution of majority- and minority-spin of Ac or Th 6d and O 2p states are all nearly symmetry. So they make almost no contribution to the magnetization. As we have seen in Table1, the Fe spin moment is very large while the Ac, Th and O spin moments are all quite small.

3.3   *Half-metallicity of $AcFe_2O_4$ and $ThFe_2O_4$ under lattice distortion*

Lattice distortion, mostly compression is often inevitably introduced in the production process and application, a small change of the lattice parameter may shift E_F (Fermi level) with respect to the half-metallic gap, which clearly affects the half-metallicity as well as the transport properties. So it is necessary to consider the influence of lattice compression on half-metallicity. First, the lattice constants of the cells of Fe_3O_4, $AcFe_2O_4$ and $ThFe_2O_4$ are reduced by 0.05 Å which we consider as compressing condition. Geometry optimization was performed on the half-metal under compressing condition so that the optimized cell under compression was got. Then the magnetic properties and electronic character were performed and ana-
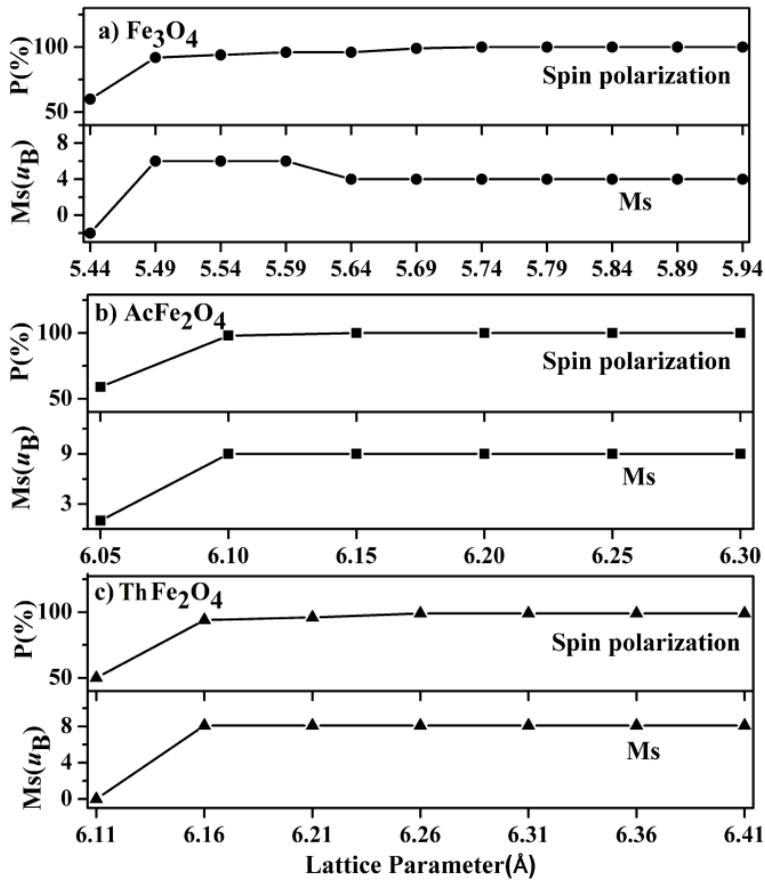
Figure 4: Molecular magnetic moments and spin polarization rate for Fe$_3$O$_4$, AcFe$_2$O$_4$ and ThFe$_2$O$_4$ as a function of lattice parameter.

lyzed. The changes of the molecular spin moments, spin-polarization of Fe$_3$O$_4$, AcFe$_2$O$_4$ and ThFe$_2$O$_4$ with lattice compression are presented in Fig.4. We can see that the spin-polarization of Fe$_3$O$_4$, AcFe$_2$O$_4$ and ThFe$_2$O$_4$ can maintain almost 100% up to 5.49 Å (-8%), 6.10 Å (-3%) and 6.16 Å (-4%), respectively at which the molecular magnetic moments all witness a sudden decrease. Especially, ThFe$_2$O$_4$, when compressed to 6.21Å, its atomic spin moments all turn into zero, which means it lose the magnetism. That is because, as the lattice parameter is decreased, 3d localization would become weaker, which can reduce the Fe spin moment. When it is decreased to a certain value, the atomic spin moments will be strongly reduced, resulting in significant magnetic losing. What is interesting

is that in 5.49 Å $\sim$ 5.59 Å region, the magnetic properties of Fe_3O_4 change significantly. A-site Fe spin changes from high and down into high and up while the B-site Fe spin becomes low and up from high and up, resulting in a 6 μ_B molecular magnetic moment compared to its 4.0 μ_B at the equilibrium lattice constant.

4   Conclusion

The half-metallicity and magnetroresistance of rare-earth metals Ac and Th doped Fe_3O_4 are investigated using DFT method. Two better half-metallic candidates for spintronic devices, i.e., $AcFe_2O_4$ and $ThFe_2O_4$ are predicted. Both of them are II B-type half-metallic materials at equilibrium lattice parameter 6.30 Å and 6.41 Å, respectively. Their molecular magnetic moments are calculated to be 8.1 μ_B and 9.0μ_B, both are much larger than that of Fe_3O_4, i.e., 4.0 μ_B. The large bonding-antibonding splitting is believed to the origin of gaps for $AcFe_2O_4$ and $ThFe_2O_4$. What's more, the half-metallicity of $AcFe_2O_4$ and $ThFe_2O_4$ cannot be affected up to 3.0% and 4% compression, respectively, while that of Fe_3O_4 can be maintained up to 8% compression. That is very important for application.

References

Born, M.; Huang, K. (1954): Dynamical Theory of Crystal Lattices. *London: Oxford University Press.*

Chen, Z. H.; Li, J. B.; Li, S. S. (2012): First principles and Monte Carlo study of Mn-doped CuCl/CuBr as room-temperature ferromagnetism materials. *J. Appl. Phys.*, vol. 111 no. 6, pp. 063913-1-063913-6.

Coey, J. M. D.; Venkatesan, M. (2002): Half-metallic ferromagnetism: Example of CrO_2(invited). *J. Appl. Phys.*, vol. 91, no. 10, pp. 8345-8350.

Dedkow, Y. S.; Rudiger, U.; Guntherodt, G. (2002): Evidence for the half-metallic ferromagnetic state of Fe_3O_4 by spin-resolved photoelectron spectroscopy. *Phys. Rev. B*, vol. 65, no. 6, pp. 064417-064421.

De Groot, R. A.; Mueller, F. M.; Van Engen, P. G.; Buschow, K. H. J. (1983): New class of materials: half-metallic ferromagnets. *Phys. Rev. Lett.* , vol. 50, no. 25, pp. 2024-2027.

Fong, C. Y.; Qian, M. C.; Pask, J. E.; Yang; L. H.; Dag, S. (2004): Electronic

and magnetic properties of zinc blende half-metal superlattices. *Appl. Phys. Lett.*, vol. 84, no. 2, pp. 239-241.

Hohenberg, P.; Kohn, W. (1964): Inhomogeneous Electron Gas. *Phys. Rev. B*, vol. 136, no. 3B, pp. B864-B871.

Hou, Y. H.; Zhao, Y. J.; Liu, Z. W.; Yu, H. Y.; Zhong, X. C.; Qiu, W. Q. (2011): First-principles investigations of Zn (Cd) doping effects on the electronic structure and magnetic properties of CoFe$_2$O$_4$. *J. Appl. Phys.*, vol. 109, no. 7, pp. 07A502-1- 07A502-3.

Kim, K. J.; Choi, S.; Lee, J. H.; Lee, H. J.; Park, J. Y. (2007): Variations of the electronic, optical and magnetic properties caused by V doping in magnetite thin films. *J. Korean Phys. Soc.*, vol. 51, no. 3, pp. 1138-1142.

Kim, W.; Kawaguchi, K.; Koshizaki, N.; Mitsugu, S.; Tetsuro, M. (2003): Fabrication and magnetoresistance of tunnel junctions using half-metallic Fe$_3$O$_4$. *J. Appl. Phys.*, vol. 93, no. 10, pp. 8032–8034.

Kohn, W.; Sham, L. J. (1965): Self-consistent equations including exchange and correlation effects. *Phys. Rev. A*, vol. 140, no. 4, pp. 1133-1138.

Kopcewicz, M.; Stobiecki, F.; Jagielski, J.; Szymanski, B.; Urbaniak, M.; Lucinski, T. (2005): Modification of microstructure and magnetic properties of Fe/Cr multilayers caused by ion irradiation. *J. Magn. Magn. Mater.*, vol. 286, pp. 437–441.

Kresse, G.; Joubert, D. (1999): From ultrasoft pseudopotentials to the projector augmented-wave method. *Phys. Rev. B*, vol. 59, no. 3, pp. 1758-1775.

Liu, J.; Chen, X. M.; Liu, Y.; Dong, H. N. (2007): First principle calculation on electronic and magnetic properties of new half-metal TiFe$_2$O$_4$. *Phys. Scr.*, vol. T129, pp. 144–148.

Liu, J.; Chen, X. M.; Liu, Y.; Dong, H. N. (2008): Electric and magnetic properties of new rare-earth half-metal LiPr$_2$O$_4$. *Solid State Ionics*, vol. 179, pp. 881–886.

Liu, J. Wang, X. Q.; Liu, Y.; Dong, H. N. (2007): First principle calculation of electric and magnetic properties for new half-metal Fe$_2$ScO$_4$. *Chin. J. Chem. Phys.* vol. 20, no. 3, pp. 291-295.

Ming, X.; Wang, X. L.; Du, F.; Han, B.; Wang, C. Z.; Chen, G. (2012): Unusual intermediate spin Fe^{3+} ion in antiferromagnetic Li$_3$FeN$_2$. *J. Appl. Phys.*, vol. 111, no. 6, pp. 063704-1-063704-6.

Prinz, G. A. (1999): Magnetoelectronics. *Science*, vol. 282, no. 5394, pp. 1660-1663.

Tan, C. L.; Huang, Y. W.; Tian, X. H.; Jiang, J. X.; Cai, W. (2012): Origin

of magnetic properties and martensitic transformation of Ni-Mn-In magnetic shape memory alloys. *Appl. Phys. Lett.*, vol. 100, no. 13, pp. 132402-1-132402-4.

Wolf, S. A.; Acoschalom, D. D.; Buhrmanm R. A.; Daughton, J. M.; von Molnár, S.; Roukes, M. L. (2001): Spintronics: a spin based electronics vision for future. *Science*, vol. 294, no. 5546, pp. 1488–1495.

Yao, Q. W.; Kimura, H.; Wang, X. L.; Konstantinov, K.; Zhao, H. Y.; Qiu, H. (2012): Density of states, magnetic and transport properties of Nd doped two dimensional perovskite compound Sr_2CoO_4. *J. Appl. Phys.*, vol. 111, no. 7, pp. 07D708-1-07D708-3.

Zhao, Y. H.; Li, Y. F.; Liu, Y. (2012): Half-metallic p-electron ferromagnetism in alkaline earth doped AlAs: A first-principles calculation. *Appl. Phys. Lett.*, vol. 100, no. 9, pp, 092407-1-092407-3.